Models for Conformationally Dynamic Metallocenes. Copolymerization Behavior of the Unbridged Metallocene (1-Methyl-2-phenylindenyl)(2-phenylindenyl)zirconium Dichloride

Michaela Dankova, Raisa L. Kravchenko, Adam P. Cole, and Robert M. Waymouth*

Department of Chemistry, Stanford University, Stanford, California 94305

Received August 17, 2001; Revised Manuscript Received January 8, 2002

ABSTRACT: The metallocene (1-methyl-2-phenylindenyl)(2-phenylindenyl)zirconium dichloride (**2**) was synthesized and its propylene homopolymerization and ethylene/propylene (EP) copolymerization behavior investigated. This metallocene yields polypropylenes of lower tacticity than the unsubstituted bis(2-phenylindenyl)zirconium dichloride (**1**). Four bridged model compounds *anti*- and *syn*-dimethylsilylbis-(2-phenylindenyl)zirconium dichloride (***anti*-3** and ***syn*-3**, respectively) and their 3-methyl-substituted analogues *anti*- and *syn*-dimethylsilyl(3-methyl-2-phenylindenyl)(2-phenylindenyl)zirconium dichloride (***anti*-4** and ***syn*-4**, respectively) were prepared to model the catalytic behavior of **2**. These studies suggest that the conformational isomer modeled by metallocene ***syn*-3** is the major contributor to the overall behavior of **2** in propylene homopolymerization. While the introduction of a methyl group onto one of the 2-phenylindenyl ligands strongly influences the structure of the resulting polypropylenes, the copolymers obtained from **2** and all four bridged metallocenes were quite similar, revealing similar copolymerization behavior for both the bridged and unbridged metallocenes.

Introduction

Considerable industrial and academic effort has been applied to develop a mechanistic understanding of polymerization catalysis for the control of polymer structure and the synthesis of polymers with tailored properties.[1,2] The properties of polyolefins are strongly dependent on their microstructure: for polypropylene, the random atactic structure is amorphous whereas stereoregular isotactic polypropylene is a high melting thermoplastic.[3] Stereoblock polypropylene consisting of alternating soft atactic and hard crystalline segments exhibits properties of a thermoplastic elastomer.[4−6]

For the past several years, we have been investigating conformationally dynamic metallocenes[7−18] as polymerization catalysts in an effort to produce block polymers[19−30] We have proposed that unbridged unsubstituted 2-arylindenyl metallocenes can change geometry during the course of a polymerization among (at least) two conformations during the polymerization reaction. Among possible rotameric forms, polymerization by the *anti*- and *syn*-like conformations, each of which inserts propylene with different selectivities,[19] could account for the production of elastomeric polypropylene with both atactic and isotactic segments in a single polymer chain (Scheme 1). Other approaches to stereoblock polymers have exploited both heterogeneous and stereorigid *ansa*-metallocene systems.[4,15,31−35]

Modifications of the 2-phenylindenyl ligand by substitution of the 2-aryl group have a dramatic influence on the stereospecificity of these catalysts.[20,21,28,36] In addition, introduction of substituents directly onto the cyclopentadienyl ring of the indenyl ligands modifies the symmetry of these complexes and leads to a conformationally rich set of accessible rotamers. We have previously found that substitution on both cyclopentadienyl rings has a deleterious effect on the productivity: the metallocene bis(1Me2PhInd)$ZrCl_2$ exhibits low productivity and low stereoselectivities and generates an amorphous polypropylene of low molecular weight.[22] However, introduction of a methyl substituent on only one of the cyclopentadienyl rings leads to an active catalyst precursor which is nonetheless much less stereospecific than the unsubstituted bis(2-phenylindenyl)zirconium dichloride/MAO catalyst system.[28]

In this contribution, we compare the propylene polymerization and ethylene/propylene copolymerization behavior of the bis(2-phenylindenyl)zirconium dichloride (**1**)/MAO catalyst system with the mixed-ring (1-methyl-2-phenylindenyl)(2-phenylindenyl)zirconium dichloride (**2**)/MAO catalyst system. The origin of the lower stereospecificity of the mixed-ring catalyst system (**2**)/MAO ([mmmm] = 14%) compared to that of (**1**)/MAO ([mmmm] = 33%) is modeled by the synthesis and study of four stereorigid metallocenes: *anti*- and *syn*-dimethylsilylbis-(2-phenylindenyl)zirconium dichloride (***anti*-3** and ***syn*-3**, respectively) and their 3-methyl-substituted analogues *anti*- and *syn*-dimethylsilyl(3-methyl-2-phenylindenyl)(2-phenylindenyl)zirconium dichloride (***anti*-4** and ***syn*-4**, respectively). In addition, the ethylene/propylene copolymerization behavior of **1**−**4** is compared and contrasted.

Results

The metallocenes (2PhInd)$_2ZrCl_2$ (**1**) and (1Me2PhInd)-(2PhInd)$ZrCl_2$ (**2**) were prepared as previously described.[28] The propylene polymerization behavior of the unbridged metallocenes **1** and **2** in liquid propylene at room temperature in the presence of MAO is given in Table 1.[28] As previously reported,[28] the stereospecificity of the methyl-substituted metallocene **2** is lower than that of **1**, yielding an amorphous polypropylene of lower tacticity and molecular weight. The polypropylene produced by **2** is amorphous and exhibits no melting transition, while that derived from **1** is elastomeric and exhibits a broad melting transition and heat of fusion ΔH = 28 J/g. Despite these marked differences in the

10.1021/ma011486m CCC: $22.00
Published on Web 03/08/2002

Scheme 1

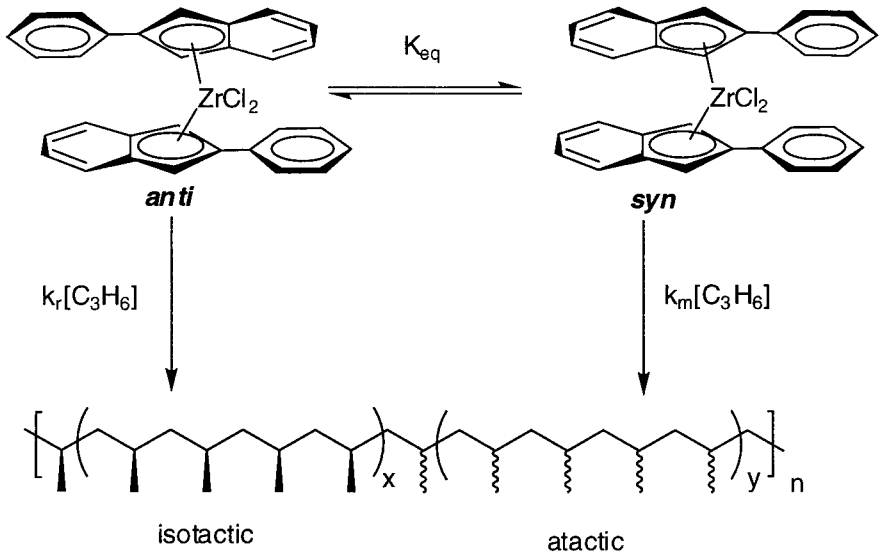

Table 1. Polypropylenes Produced with 1 and 2[a]

	$(2PhInd)_2ZrCl_2$ (**1**)	(1Me2PhInd)(2PhInd)$ZrCl_2$ (**2**)
% [mmmm][b]	33	14
productivity[c]	3030	2800
M_w ($\times 10^{-3}$)[d]	542	293
MWD[d]	3.5	3.77
T_m (°C)[e]	30−152	
ΔH_m (J/g)[e]	28	

[a] Kravchenko, R. L. Ph.D. Thesis, Stanford University, 1997. [b] By ^{13}C NMR. [c] In kg of PP/(mol of Zr h). [d] By high-temperature GPC vs polypropylene standards. [e] By differential scanning calorimetry.

stereospecificity of the two metallocenes, the productivities of both compounds are comparable.

Unbridged metallocene **2** can adopt several stable conformations that can in principle contribute to the overall polymerization behavior (Figure 1). In an effort to model these conformations, the stereorigid *ansa*-metallocenes *anti*- and *syn*-dimethylsilylbis(2-phenylindenyl)zirconium dichloride (***anti*-3** and ***syn*-3**, respectively) and the 3-methyl-substituted analogues *anti*- and *syn*-dimethylsilyl(3-methyl-2-phenylindenyl)(2-phenylindenyl)zirconium dichloride (***anti*-4** and ***syn*-4**, respectively) were prepared.

The synthesis of ***anti*-3** and ***syn*-3** was carried out according to the published procedure.[23] Both ***anti*-4** and ***syn*-4** were synthesized by a procedure similar to that reported by Collins.[35] The ligand 1-methyl-2-phenylindene was prepared by a previously published procedure,[22] deprotonated by *n*-butyllithium, and reacted with dichlorodimethylsilane in THF to produce 3-methyl-2-phenylindenylchlorosilane. The resulting 3Me2PhIndMe$_2$SiCl was then treated with the lithium salt of 2-phenylindene in THF to give two isomers of the ligand which were deprotonated using 2 equiv of *n*-butyllithium and reacted further with zirconium tetrachloride in a diethyl ether/pentane mixture (Scheme 2). After stirring under an argon atmosphere for 10 h, an orange solid was isolated by filtration of the mixture. The resulting orange powder was recrystallized from methylene chloride to obtain pure ***anti*-4**.

The pure ***syn*-4** isomer was isolated by repeated recrystallization of the dried filtrate of the original reaction from THF, toluene, and methylene chloride. The purity of both catalysts was confirmed by elemental analysis and by ^1H NMR.[37] Yields of ***anti*-4** and ***syn*-4** based on unoptimized reaction conditions were 4% and 1%, respectively.

Owing to the C_1 symmetric nature of the ligand framework, the identities of both bridged metallocenes **4** could not be unambiguously assigned using ^1H NMR. Both *anti*- and *syn*-isomers show two sets of resonances in the methylsilyl region. We used 2D COSY NMR to assign the phenyl and indenyl resonances in the aromatic region of the ***syn*-4** metallocene. NOE difference spectroscopy revealed dipolar interactions between the silyl methyl protons of the bridging group and the indenyl and/or phenyl protons of the ligand. We identified the ***syn*-4** catalyst by observing enhancement of the indenyl protons when irradiating one silyl methyl signal and enhancement of the phenyl protons when irradiating the other silyl methyl resonance. This assignment was confirmed by the X-ray crystal structure of the methyl derivative ***anti*-4b** (vida infra).

X-ray Crystal Structure. Crystals of the unbridged metallocene **2** were grown out of toluene solution at −20 °C. The X-ray structure (Figure 2) reveals that the compound crystallizes in an *anti*-conformation with the 1-methyl substituent oriented approximately above one of the chlorine ligands. Representative bond lengths and angles are tabulated in Table 3. The bond distances and angles are typical for unbridged metallocenes of this class.[19,20,38] A notable difference between the structure of **2** and the unsubstituted **1** are the dihedral angles between planes defined by the phenyl and indenyl rings. For **1**, these dihedral angles are less than 10°; for **2** the dihedral angle is 31° for plane 1/plane 2 and 25° for plane 3/plane 4 (as defined in Table 3). We had previously suggested that the deviance of this dihedral angle from 0° might be a consequence of the substituent on the 1-position of the ligand (either the 1-methyl substituent[22] or a silicon bridge[23]). The fact that the dihedral angle for planes 1 and 2 (see Table 3) is 25° suggests that the small dihedral angles between the phenyl and indenyl planes observed in a number of other crystal structures containing 2-arylindene ligands does not necessarily reflect a strong electronic bias toward conjugation of the phenyl ring with the indenyl ligand.[19,20,24,28,38]

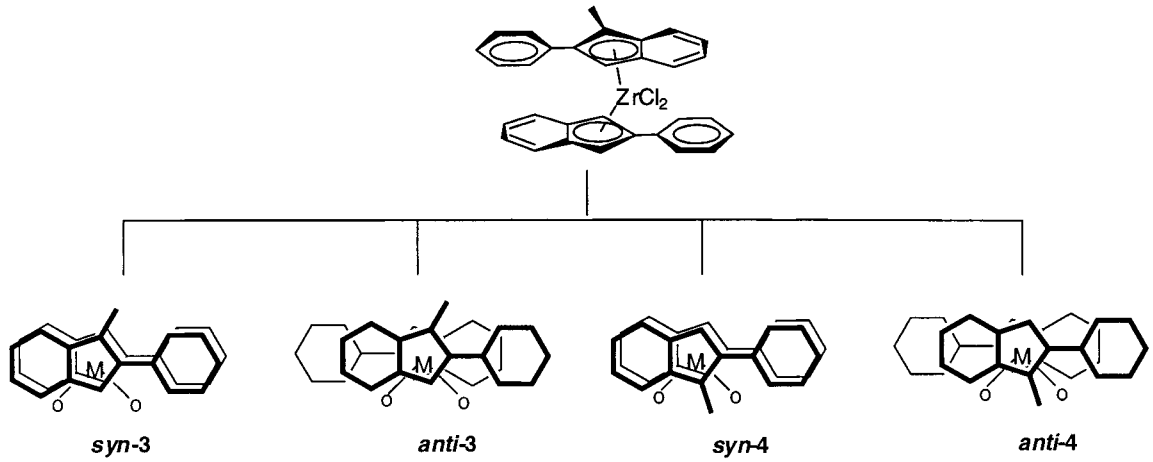

Figure 1. Rotameric forms of **2**.

Scheme 2

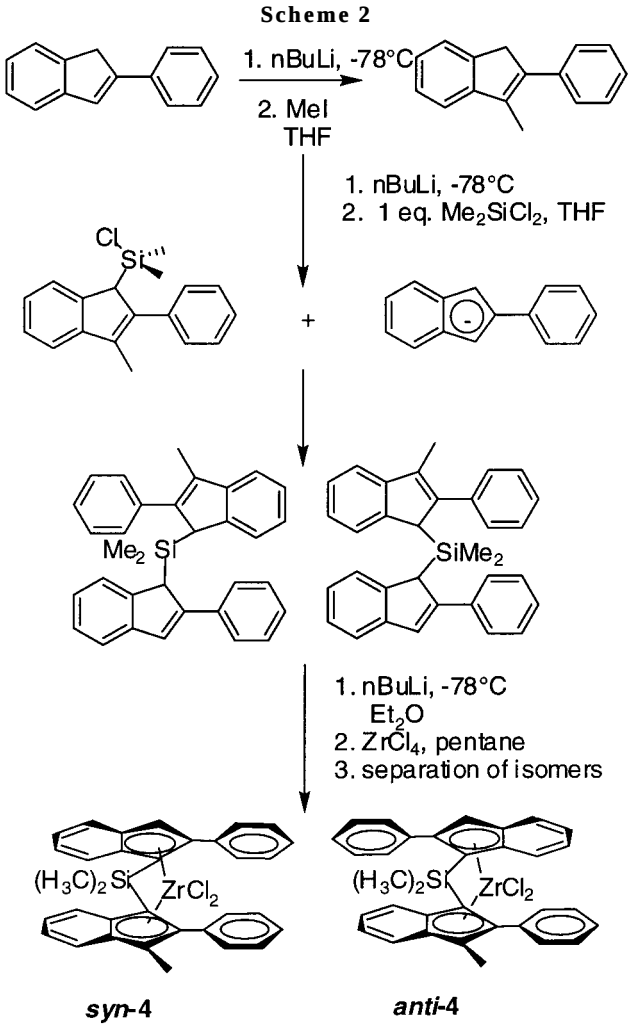

***Anti*-4** is only sparingly soluble in most organic solvents, and attempts at obtaining X-ray quality crystals were unsuccessful. Therefore, ***anti*-4** was methylated, and crystals were grown out of methylene chloride/pentane mixture at room temperature. Analysis of the structure reveals a superposition of $LZr(CH_3)_2$ with $LZr(CH_3)(Cl)$ in an approximate 7:3 ratio (Figure 3). The partial occupancy of the methyl ligand does not allow a careful comparison of the Zr−Me or Zr−Cl bond distances or angles; nevertheless, the crystal structure of ***anti*-4b** reveals that the geometry and bonding of this complex was similar to that observed for the unbridged

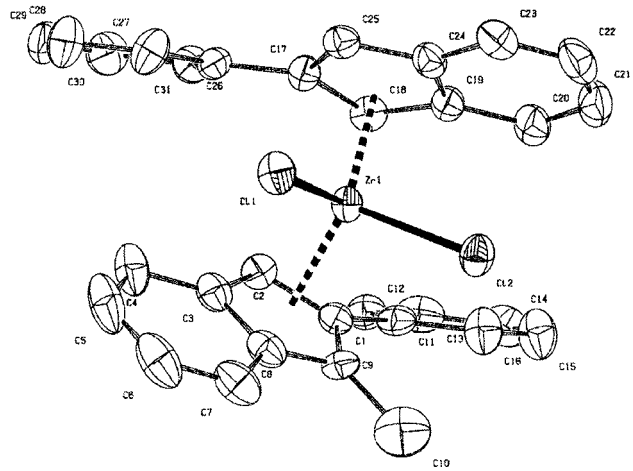

Figure 2. Solid-state structure of **2**.

complex (1Me2PhInd)(2PhInd)$ZrCl_2$ (**2**) (Table 3). Constraining the two portions of the ligand by a bridge results in slightly smaller Cp(centroid)−Zr−Cp(centroid) angle (128.7°) when compared to the unbridged **2** (130.6°), as previously observed for **syn-3**.[23] The most obvious difference between the bridged and unbridged metallocenes is the difference in the magnitude of the dihedral angles between the plane of the phenyl and indenyl portion of the ligands (44° and 61° for the *ansa*-metallocene ***anti*-4b** and 25° and 31° for unbridged metallocene **2**). Similar dihedral angles have been observed in the X-ray crystal structure of ***syn*-3**.[23]

Propylene Polymerization. The mixed-ring metallocene **2**/MAO polymerizes propylene to an amorphous polypropylene with low tacticity ([mmmm] = 14%).[28] The polypropylene polymerization behavior of ***anti*-3** and ***syn*-3** had been previously reported; the results for these three metallocenes are summarized in Table 2.[23] Propylene polymerization with both ***anti*-4** and ***syn*-4** was carried out under similar conditions to that reported for **1**, **2**, ***anti*-3**, and ***syn*-3** in liquid propylene at 20 °C in the presence of MAO. Under these conditions, both ***anti*-4** and ***syn*-4** yield polypropylenes with isotactic pentad contents in the range of [mmmm] = 54−62%; the pentad distributions of these polymers (see Supporting Information) yield isolated rr triad as the predominant stereoerrors. The productivities of metallocene ***syn*-4** were quite variable. This metallocene was also observed to be quite thermally labile in solution as well as in solid state; thus, this variability may be a

Table 2. Propylene Homopolymerization with *ansa*-Metallocenes *anti*-3, *anti*-4 and *syn*-3, *syn*-4[a]

entry	catalyst	prod[b]	[mmmm][c] (%)	M_n ($\times 10^{-3}$)[d]	MWD[d]	T_m (°C)[e]	ΔH (J/g)[e]
1	(**2**) (1Me2PhInd)(2PhInd)$ZrCl_2$[f]	2800	14	78	3.77		
2	(***anti*−4**) *anti*-Me_2Si(3Me2PhInd)(2PhInd)$ZrCl_2$	1240	57	100	2.1	38−155	51
3		1120	54	n.d.	n.d.		
4		1272	53	96	2.1		
5	(***syn*−4**) *syn*-Me_2Si(3Me2PhInd)(2PhInd)$ZrCl_2$	1545	61	53	1.9	35−110	50
6		951	63	46	1.9		
7		2901	62	n.d.	n.d.		
8		2258	60	n.d.	n.d.		
9	(***anti*−3**) *anti*-$Me_2Si(2PhInd)_2ZrCl_2$	2408	86	167	2.6	n.d.	n.d.
10		2327	87	133	3.1		
11		2573	88	n.d.	n.d.		
12	(***syn*−3**) *syn*-$Me_2Si(2PhInd)_2ZrCl_2$	4092	7	n.d.	n.d.	n.d.	n.d.
13		3951	6.2	61	2.0		
14		4058	6.2	88	2.2		

[a] Conditions: 100 mL of liquid propylene/20 mL of toluene, T_p = 20 °C, time = 20 min, [MAO] = 100 mg, [Zr] = 5×10^{-5} M. [b] In kg of PP/(mol of Zr h). [c] By ^{13}C NMR. [d] By high-temperature GPC vs polypropylene standards. [e] By differential scanning calorimetry. [f] Tagge, C. D.; Kravchenko, R. L.; Tappan, K. L.; Waymouth, R. M. *Organometallics* **1999**, *18*, 380−388.

Table 3. Selected Bond Lengths (Å) and Bond Angles (deg) for Complexes *anti*-4, 2, and *syn*-3

	anti-Me_2Si-(1Me2PhInd)-(2PhInd)Zr-(Cl)Me (***anti*−4b**)	*rac*-(1Me2PhInd)-$(2PhInd)_2$-$ZrCl_2$ (**2**)	*syn*-Me_2Si-$(2PhInd)_2$-$ZrCl_2$ (***syn*−3**)[d]
Cl−Zr−Cl		95.37	94.41
Cl−Zr−Me	85.76		
Zr−Cl	2.61	2.45	2.41
		2.42	2.44
Zr−Me	2.28		
Zr−Me(Cl)[a]	2.19		
Zr−plane 1	2.25	2.24	2.23
Zr−plane 3	2.26	2.25	2.22
plane 1−Zr−plane 3	128.5	130.6	125
plane 1/plane 2[b]	43.95	25	50
plane 3/plane 4[c]	61.03	31	60

[a] The distance reported in the table corresponds to the Zr−Me distance; the position of Me substituent is fractionally occupied by Cl atom in a ratio Me:Cl = 7:3 (see text). [b] Plane 1 = C1−C2−C7−C8−C9 (***anti*-4b**), C17−C18−C19−C24−C25 (**2**), C1−C2−C3−C4−C9 (***syn*-3**); plane 2 = C10−C11−C12−C13−C14−C15 (***anti*-4b**), C26−C27−C28−C29−C30 (**2**), C10−C11−C12−C13−C14−C15 (***syn*-3**). [c] Plane 3 = C16−C17−C22−C23−C24 (***anti*-4b**), C1−C2−C3−C8−C9 (**2**), C16−C17−C18−C19−C24 (***syn*-3**); plane 4 = C25−C26−C27−C28−C29−C30 (***anti*-4b**), C11−C12−C13−C14−C15−C16 (**2**), C25−C26−C27−C28−C29−C30 (***syn*-3**). [d]Maciejewski Petoff, J. L.; Agoston, T.; Lal, T. K.; Waymouth, R. M. *J. Am. Chem. Soc.* **1998**, *120*, 11316−11322.

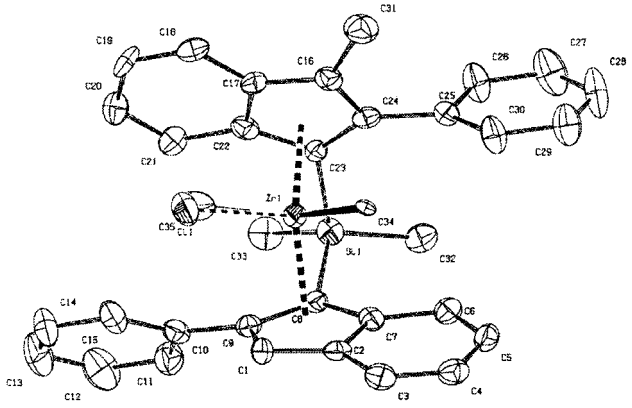

Figure 3. Solid-state structure of **anti-4b**.

consequence of catalyst decomposition.[37] Nevertheless, the data suggest that the productivities for both ***syn*-4** and ***anti*-4** are lower than those of the other metallocenes investigated (**1**, **2**, ***anti*-3**, and ***syn*-3**). The number-average molecular weights of the polypropylenes produced by ***syn*-4** are low at approximately 50 000 g/mol and approximately half that produced by ***anti*-4** (100 000 g/mol). For both **3** and **4**, the *syn*-isomers produced lower molecular weights than the *anti*-isomers (Table 2).

Ethylene/Propylene Copolymerization. Ethylene and propylene were copolymerized using metallocene **2** and all four bridged metallocenes ***anti*-3**, ***syn*-3**, ***anti*-4**, and ***syn*-4**. Copolymerizations were carried out in 100 mL of liquid propylene with constant overpressure of ethylene at 20 °C. Propylene conversion was kept to ≤10% with less than 3 g of polymer produced to avoid drift in composition of the monomer mixture. The ratio of the mole fraction of ethylene and propylene in the liquid phase (X_e/X_p) was determined using gas fugacities as described by Kravchenko.[26]

The molecular weight of the EP copolymer produced from the *syn*-like isomers is lower that the *anti*-analogues at similar ethylene incorporation. The polydispersities of the polymers obtained from bridged metallocenes are approximately 2−3 with **anti-3** yielding slightly higher polydispersity, M_w/M_n = 3.8−5.1 (Table 4).

The distribution of diads and triads of the comonomer sequence was determined from quantitative ^{13}C NMR of the copolymers.[39] Comparison of triads at approximately 40% ethylene (see Supporting Information) show that all four catalysts ***anti*-4**, ***syn*-4** and ***anti*-3**, ***syn*-3** produce copolymers with similar triad distributions.

The reactivity ratios, $r_e = k_{ee}/k_{ep}$ and $r_p = k_{pp}/k_{pe}$, are defined according to the first-order Markov copolymerization mechanism[40] as the ratio of the rate constant of the homopropagation step to the rate constant for the cross-propagation step. All four bridged catalysts show a similar and relatively high tendency to incorporate propylene with r_e's in the range of r_e = 2.6−6.0 and r_p = 0.16−0.20. The product of reactivity ratios ($r_e r_p$), determined from diads using method developed by Kakugo,[39] is an indirect measure of the monomer distribution along a polymer chain. The product $r_e r_p$ = 0.5−0.7 for ***anti*-3** and ***anti*-4** suggests a tendency of these catalysts to produce random EP copolymer with a slight bias toward alternating distribution of monomers. ***Syn*-3** and ***syn*-4** show $r_e r_p$ = 0.8−1.0, indicative of a statistical distribution of monomers along the polymer chain. The metallocenes ***anti*-4**, ***syn*-4** and ***anti*-3**, ***syn*-3** all produce amorphous copolymers in the range of comonomer contents investigated and show no evidence of a melting transition by differential scanning calorimetry.

Table 4. Ethylene/Propylene Copolymerization Parameters for *ansa*-Metallocenes *anti*-3, *anti*-4 and *syn*-3, *syn*-4[a]

N_{exp}[b]	metallocene	X_e/X_p in feed[c]	% E in polymer[d]	avg prod[e]	$r_e r_p$[f]	r_e[f]	r_p[f]	M_n ($\times 10^{-3}$)[g]	MWD[g]
5	**(1)**[h]	0.065	25		1.3 ± 0.20	5.4 ± 0.9	0.24 ± 0.04	688	2.6
4	**2**	0.132−0.136	44−45	30000	1.33 ± 0.20	7.23 ± 0.21	0.18 ± 0.02	281	3.5
2		0.064	25−27		1.27	7.12 ± 0.39	0.18 ± 0.02	65	4.2
3	**(*anti*−4)**	0.134	35−40	3000	0.65 ± 0.03	3.74 ± 0.36	0.18 ± 0.02	n.d.	n.d.
2		0.062	23		0.78 ± 0.09	4.35 ± 0.33	0.18 ± 0.01	67	3.0
3	**(*syn*−4)**	0.134	37−40	3000	0.96 ± 0.05	4.81 ± 0.36	0.20 ± 0.01	47	3.1
2		0.062	21−24		1.27 ± 0.08	6.46 ± 0.51	0.20 ± 0.01	55	2.9
2	**(*anti*−3)**	0.132−0.137	34−38	3500	0.53	2.64 ± 0.15	0.20 ± 0.01	66	3.8
3		0.062	21−22		0.62 ± 0.10	2.99 ± 0.42	0.20 ± 0.03	54	5.1
3	**(*syn*−3)**	0.136−0.137	39−41	2000	0.79 ± 0.05	4.83 ± 0.34	0.16 ± 0.01	44	2.1
2		0.062−0.062	22		1.08 ± 0.06	6.00 ± 0.31	0.18 ± 0.01	54	2.0

[a] Conditions: 100 mL of liquid propylene/20 mL of toluene, T_p = 20 °C, time = 20 min, [Zr] = (1−10) × 10^{-6} M, MAO = 130 mg. [b] Number of experiments used for determination of the average reactivity ratios. [c] The range of the ratios of the mole fractions of ethylene (X_e) and propylene (X_p). [d] The range of mol % E in copolymers determined using ^{13}C NMR. [e] In kg of PE/(mol of Zr h), averaged over several runs; see Supporting Information. [f] Determined using ^{13}C NMR and diads equations according to Kakugo. [g] Determined by high-temperature GPC. [h] Kravchenko, R.; Waymouth, R. M. *Macromolecules* **1998**, *31*, 1−6.

Discussion

Unbridged indenyl metallocenes are conformationally dynamic systems that are capable of generating several distinct catalytically active conformations during the course of a polymerization reaction.[7,10,11,13,17−20,22,38,41−43] The polymerization behavior of such conformationally dynamic metallocenes and the structure of the resulting polymer depend on the accessible metallocene conformations and the rate at which these conformers interconvert relative to the rate at which they insert monomer.[30,44] The challenge in studying these fluxional catalysts arises from the fact that several catalyst conformations of different stabilities, reactivities, and selectivities are likely to be involved in polymerization. It is in general difficult to establish which conformations contribute to the polymerization behavior. Dynamic NMR measurements can provide useful information on accessible conformations and their rates of interconversion,[11,14,38,41,45] and kinetic models can be applied to estimate the relative role of the various assumed conformations as well as their dynamics.[30]

The role of various conformations can also be usefully interrogated through the synthesis and study of stereorigid metallocenes that are locked into conformations representing accessible rotameric forms of the unbridged catalyst.[23,46] The choice of conformationally locked metallocenes is guided by computational studies of accessible conformations[42,43] as well as X-ray data of metallocene catalyst precursors.[19,20,47] The synthesis of a stereorigid metallocene necessarily requires the introduction of a bridging group, and the presence and nature of a bridging group can have an influence on the reactivity of metallocene complexes.[48,49] Nevertheless, while it must be appreciated that these model complexes can only provide indirect support for the role of the various conformations, the study of these rigid conformers can provide fundamental information about polymerization behavior of coordination geometries that can be accessed by these conformationally dynamic systems. Computational studies[42,43,50] have shown that for $(2PhInd)_2ZrCl_2$ (**1**) there are two conformational minima corresponding to *anti*- and *syn*-geometries of the catalyst. Both conformers were also found in a single crystal of the catalyst corroborating similar stability of these two rotameric forms of **1** in the solid state.[19]

In addition to providing fundamental information on the polymerization behavior of conformationally dynamic systems, these mechanistic studies are also a valuable tool to interpret the effects of ligand modifications on the stereospecificity of this class of metallocenes. In this paper we attempt to address the origin of the lower stereoselectivity of the methyl-substituted metallocene $(1Me2PhInd)(2PhInd)ZrCl_2$ (**2**) compared to that of bis(2-phenylindene)zirconium dichloride (**1**) (**1**, [mmmm] = 33%; **2**, [mmmm] = 14%, Table 1). One of the intriguing consequences of the lower symmetry of **2** relative to **1** is that even if we assume only the *syn*- and *anti*-rotamers as accessible conformational states (as suggested by Rappe[42] and Guerra[43]) metallocene **2** has four accessible conformations compared to only two for **1** (Figure 1). In an effort to model the polymerization behavior of **2**, we have compared the solid-state structure and polymerization behavior of **2** to four stereorigid *ansa*-metallocenes ***anti*-3**, ***syn*-3**, ***anti*-4**, and ***syn*-4**.

Synthesis and Structure. Metallocenes **2**, ***anti*-3**, and ***syn*-3** were prepared as previously described.[23,28] The synthesis of metallocenes ***anti*-4** and ***syn*-4** (Scheme 2) was carried out by a procedure analogous to that reported by Collins[35] to yield both ***anti*-4** and ***syn*-4** in very low yield. These metallocenes are quite unstable both in solution and in the solid state,[37] and their polymerization behavior was investigated within 4 days of their isolation and crystallization. The crystal structure of **2** reveals an *anti*-conformation with 2-phenyl rings displaced on opposite sides of the metallocene and the methyl group oriented over one the coordination sites approximately parallel to one of the Zr−Cl bond vectors. This conformation is analogous, albeit slightly twisted relative to that observed for silicon-bridged analogue ***anti*-4b**.

Propylene Homopolymerization. The results of the propylene polymerizations with the unbridged metallocene **2** and the bridged metallocenes **3**−**4** are reported in Table 2. As previously reported, the metallocene ***syn*-3** is approximately twice as productive as ***anti*-3**; the data for ***syn*-4** and ***anti*-4** show a similar trend, although we observed variable productivities for ***syn*-4** which we attribute to its thermal instability. These observations are in contrast to most literature reports[47,51−54] where the *anti*-isomer of bridged metallocenes are more productive than the *syn*. It seems reasonable to assume that the bulky substituent in the 2-position of the ligand causes the productivity trends observed here, effectively making ***anti*-3** and ***anti*-4** more sterically hindered than both the *syn*-isomers.

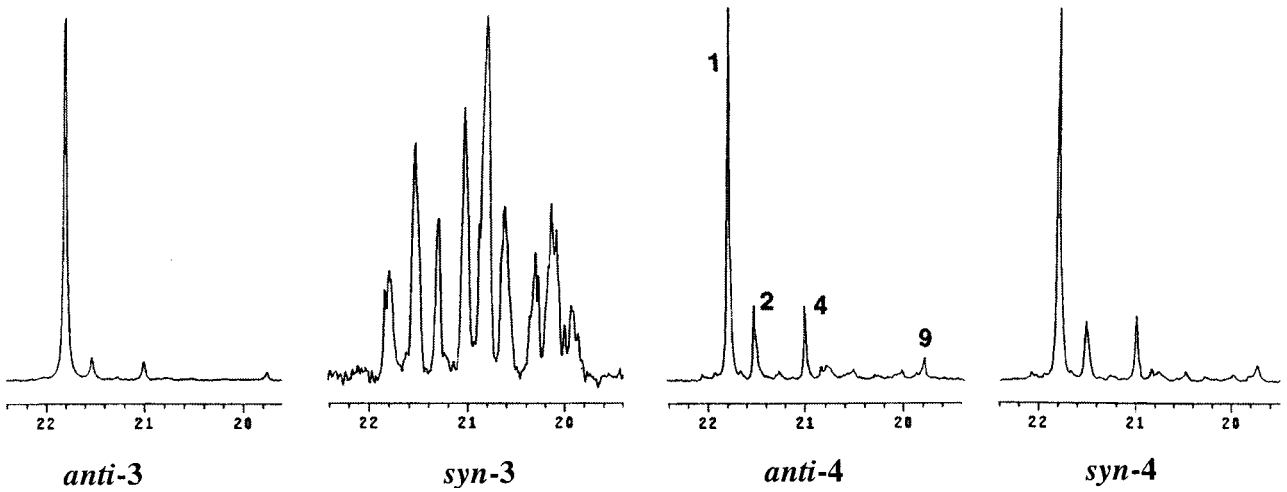

Figure 4. ^{13}C NMR spectra of methyl region of polypropylenes (1 = [mmmm], 2 = [mmmr], 4 = [mmrr], 9 = [mrrm]).

Scheme 3

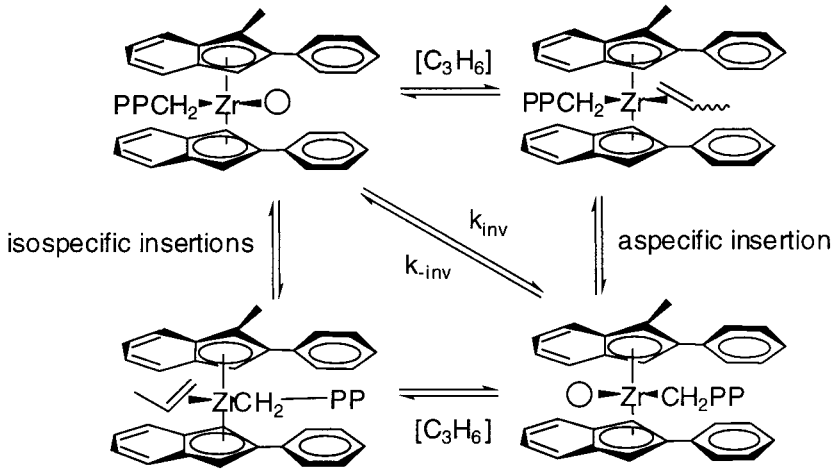

The trends observed in the catalysts' productivities are opposite those observed in polymer molecular weights. ***Anti*-3** and ***anti*-4** produce polymers of almost twice the molecular weight of their *syn*-analogues. Similar trends in molecular weight were observed by Collins and co-workers for *syn*-$Me_2Si(3MeInd)(Ind)ZrCl_2$ (***syn*-5**) and *anti*-$Me_2Si(3MeInd)(Ind)ZrCl_2$ (***anti*-5**), but the introduction of the 2-phenyl substituent leads to much higher molecular weights for the polypropylenes. Even accounting for the different polymerization conditions (45 psi of propylene over toluene[35] vs liquid propylene), the molecular weights of the 2-phenyl-substituted *ansa* metallocenes ***syn*-4** and ***anti*-4** (M_n = 45 000 and 96 000, respectively) are considerably higher than ***syn*-5** and ***anti*-5** (M_n = approximately 880 and 36 700, respectively).[35]

The stereospecificity of the bridged metallocenes depends sensitively on their substitution pattern and symmetry. As previously reported,[23] ***anti*-3** produces highly isotactic polypropylene with [mmmm] = 87% whereas the achiral ***syn*-3** produces atactic polypropylene ([mmmm] = 7%). In contrast, both ***anti*-4** and ***syn*-4** produce similar polypropylenes of intermediate tacticity with [mmmm] ranging from 54 to 62%. The pentad distribution for both ***anti*-4** and ***syn*-4** (see Supporting Information) reveals that the predominant stereoerrors are associated with [mmmr], [mmrr], and [mrrm] pentads (Figure 4). The stereospecificity of ***anti*-4** and ***syn*-4** is similar to but higher than that observed by Collins[35] for the analogous *ansa*-metallocenes ***syn*-5** and ***anti*-5** which lack a 2-phenyl substituent. One explanation for the intermediate tacticities for the polypropylenes produced by the *ansa*-metallocenes ***syn*-4** and ***anti*-4** is that these unsymmetrical metallocenes possess both a stereoselective and a nonstereoselective state and that the states can interconvert either by monomer insertion or by inversion at the metal center (Scheme 3). This type of mechanism has been discussed for a variety of C_1-symmetric metallocenes[15,33,55−62] and was subject to a recent detailed analysis by Collins and co-workers.[35,49] According to this scheme, the alternate insertion of monomers at the stereoselective and nonstereoselective site would lead to hemi-isotactic polypropylene ([mmmm] = 19%);[56,57] the higher tacticities observed for ***anti*-4** and ***syn*-4** could thus be explained by competitive isomerization at the metal site (with more frequent insertion into the isospecific site) in competition with olefin insertion, as suggested by Collins for ***syn*-5** and ***anti*-5**.[35] Further details on the propylene polymerization behavior of ***anti*-4** and ***syn*-4** will be the subject of a future publication.[63]

Implications for the Stereospecificity of 2. The unbridged metallocene **2** generates a lower-tacticity polypropylene ([mmmm] = 14%) than the unsubstituted metallocene $(2\text{-PhInd})_2ZrCl_2$ (**1**), under comparable polymerization conditions.[28] We had envisaged two possible explanations for the lower stereoselectivity of **2**

relative to **1**: (a) the introduction of the methyl substituent on the 2-phenylindene ligand might force the metallocene to adopt a conformation that is less stereospecific, or (b) the catalyst derived from **2** might populate four (or more) conformations whose aggregate behavior leads to low-tacticity polypropylene. With regard to the first possibility, the crystal structure of **2** indicates that a conformation with the methyl group displaced out over the coordination sphere is a stable and accessible conformation; however, the observation that both ***anti*-4** and ***syn*-4** yield polypropylenes with tacticities above [mmmm] = 50% implies that neither of these rotameric forms contributes significantly to the polymerization behavior of the unbridged metallocene **2**.[64]

With regard to possibility (b), the aggregate behavior of a conformationally dynamic system will depend on the number of accessible conformations, their relative stabilities, their relative rates of propagation, and their rates of interconversion relative to propagation.[30] These conformations can (i) interconvert faster than the rate of propagation (Curtin−Hammet conditions), (ii) interconvert at about the same rate producing short blocks of different tacticity, and (iii) interconvert slower than chain lifetime resulting in a blend of chains of different tacticity. The lower stereospecificity of **2** relative to **1** might then be attributed to one of two limiting possibilities: (I) the accessible conformations are of similar stabilities and activities but interconvert at a rate faster than propagation, leading to a random microstructure, or (II) the conformation modeled by ***syn*-3**, which yields atactic polypropylene, is the dominant contributor to the polymerization behavior of **2** (i.e., is either the most stable or the conformation with the highest rate of propagation). At the present time, we do not have any information to assess the relative stabilities of the conformations modeled by metallocenes ***anti*-3**, ***syn*-3**, ***anti*-4**, and ***syn*-4** (Figure 1) or the rates of interconversion relative to propagation. Thus, we have no data which allow us to unambiguously descriminate between possibilities (I) and (II). Nevertheless, the higher productivities observed for ***syn*-3** relative to the other bridged isomers is consistent with its being the most reactive conformer.

Ethylene/Propylene Copolymerization. The copolymerization of ethylene and propylene was carried out with the unbridged metallocene **2** and the *ansa*-metallocenes **3** and **4** both to further investigate the polymerization behavior of conformationally dynamic metallocenes and to try to assess the role of conformational dynamics and ligand architecture on the copolymerization behavior of indenyl metallocenes. The results of these copolymerizations are tabulated in Table 4. For these studies, the range of ethylene incorporation was confined to 21−45% ethylene in the copolymers due to safety considerations associated with our experimental procedure.[65]

The productivity of the unbridged metallocene **2** was observed to be almost an order of magnitude higher than the bridged complexes (see Supporting Information); this observation and the variable productivities observed for metallocenes **3** and **4** may be a consequence of the poor stability of some of the bridged metallocenes. The number-average molecular weights of the EP copolymers were comparable at approximately 60 000 (except for one run with **2** which gave a M_n = 281 000) and the molecular weight distributions broader than M_w/M_n = 2.0 for all metallocenes except for ***syn*-3**.

The copolymerization parameters for metallocenes **2**−**4**, determined by the method of Kakugo,[39] are given in Table 4. The unbridged metallocene **2** shows a very good tendency to incorporate propylene comonomer, as evidenced by a relatively low r_e = 7.2 and a relatively high r_p = 0.18. Similar behavior was recently reported for the unsubstituted $(2PhInd)_2ZrCl_2$ (r_e = 5.4, r_p = 0.24)[26] and is unusual for unbridged metallocenes. It has been reported in the literature[66] that unbridged metallocenes are poor at incorporating comonomer, as evidenced by the behavior of the unbridged metallocenes, $(Cp)_2ZrCl_2$ and $(Ind)_2ZrCl_2$ for which r_e = 29 and 25, respectively, and r_p = 0.09 and 0.03, respectively.[66] Our experience with the unbridged 2-arylindenylmetallocenes suggests that this copolymerization behavior is not simply a consequence of the presence or absence of a bridging group; we find unbridged metallocenes with the appropriate substitution pattern can be quite promiscuous toward α-olefin comonomers.[26,67] The bridged 2-arylindenyl metallocenes show similarly good incorporation of propylene, implicating that some factor other than a bridging group is responsible for the high propylene selectivity.

The copolymerization characteristics of the bridged metallocenes **3** and **4** are quite similar, despite their different coordination geometries, with r_e's in the range 2.6−6.4 and r_p's in the range 0.16−0.20. These copolymerization parameters are comparable to those reported for *rac*-$Me_2Si(Ind)_2ZrCl_2$ (r_e = 4.23 and r_p = 0.12).[66] The observation that the copolymerization characteristics of ***syn*-3**/***syn*-4** and ***anti*-3**/***anti*-4** are so similar was something of a surprise to us, especially in light of their quite different propylene stereoselectivities. We had anticipated that incorporating a methyl group onto the 3-position of these bridged metallocenes would have an influence on the relative kinetic selectivities toward ethylene and propylene. This is apparently not the case for this class of C_1-symmetric metallocenes and can be contrasted to our own[27] and others'[68] investigations of the C_1-symmetric $Me_2C(RCp)$-(fluorenyl)$ZrCl_2$ metallocenes, where introduction of a methyl group (R = Me vs R = H) dramatically alters the copolymerization behavior and leads to alternating EP copolymers.

The sequence distributions of the olefin copolymers produced by metallocenes **2**−**4** are Markovian and close to ideal (i.e., random distributions), as manifested in products of reactivity ratios $r_e r_p$ which span $r_e r_p$ = 1.[40] For this particular class of metallocenes, the similarities of the copolymerization behaviors for the unbridged metallocene **2** and the *ansa*-metallocenes **3** and **4** do not allow us to use the copolymerization characteristics of the bridged metallocenes **3** and **4** to interpret the copolymerization behavior of the conformationally dynamic metallocene **2**. Nevertheless, these studies have illuminated some of the limits of our understanding on the role of substituent effects on copolymerization behavior (i.e., ***syn*-3** vs ***syn*-4** and ***anti*-3** vs ***anti*-4**) in addition to providing insight into the stereospecificity of conformationally dynamic catalysts.

Conclusions

In summary, we have prepared four stereorigid analogues of the fluxional $(1Me2PhInd)(2PhInd)ZrCl_2$ system to establish the propylene polymerization behavior of four rotameric forms of the unbridged catalyst

2. The polypropylene stereostructure is significantly affected by introduction of the methyl substituent in the case of ***anti*-4** and ***syn*-4** that produce polypropylene with isotactic pentad content [mmmm] = 53−63%. In contrast, ***anti*-3** produces isotactic polypropylene and ***syn*-3** produces atactic polypropylene. The combination of the tacticity, productivity, and molecular weight data suggests that propylene homopolymerization behavior of fluxional mixed ligand catalyst **2** is a consequence of either (I) competitive rates of insertion and isomerization of rotameric forms leading to more random microstructures or (II) that the *meso*-like rotamer modeled by the ***syn*-3** isomer is the predominant isomer contributing to the polymerization behavior of the unbridged **2**.

For EP copolymerization all catalysts ***anti*-3**, ***anti*-4** and ***syn*-3**, ***syn*-4** display similar copolymerization parameters. The methyl substituent of ***anti*-4** and ***syn*-4** strongly influences the catalysts' behavior in the homopolymerization of propylene; however, it does not seem to have a distinct effect on the copolymerization characteristics. The differences in the reactivities toward ethylene and propylene of the four modeled rotamers of the unbridged catalyst **2** are so small that the four rotameric forms produce copolymers of similar random sequence distributions.

It is conceivable that coordination geometries other than those modeled here may contribute to the polymerization behavior of unbridged 2-arylindenylmetallocenes, and work is being carried out in our group to investigate the possible contribution of additional rotameric forms to the overall behavior of 2-arylindenyl zirconocenes. Other means of introducing fluxional behavior into a catalyst and thereby controlling copolymerization process are also under investigation.

Experimental Section

General Consideration. All organometallic reactions were conducted using standard Schlenk and drybox techniques. Elemental analyses were performed by E&R Microanalytical Laboratory. Diethyl ether and tetrahydrofuran (THF) were distilled from sodium/benzophenone ketyl. Methylene chloride and pentane were distilled from calcium hydride prior to use. Toluene was passed through two purification columns packed with activated alumina and supported copper catalyst and collected under argon. Chloroform-d_3 was vacuum transferred from calcium hydride. Benzene-d_6 was vacuum transferred from sodium benzophenone. 2-Phenylindene, *n*-butyllithium (^{n}BuLi), and dichlorodimethylsilane (Me_2SiCl_2) were purchased from Aldrich. Zirconium tetrachloride ($ZrCl_4$) was purchased from Fluka. NMR spectra were recorded on a Varian Gemini 400 MHz, Varian UI 300 MHz, and UI 500 MHz spectrometer. 3-Methyl-2-phenylindene, (1-methyl-2-phenylindenyl)(2-phenylindenyl) zirconium dichloride, and *anti*- and *syn*-bis(2-phenylindenyl)zirconium dichloride were prepared according to literature procedures.

3-Methyl-2-phenyl-1-chlorodimethylsilylindene. 3-Methyl-2-phenylindene (2.2 g, 10.66 mmol) was weighed into a dry Schlenk flask and diluted with 80 mL of THF. This solution was cooled to −78 °C, treated with ^{n}BuLi (2.5 M in hexanes, 10.98 mmol) slowly via syringe, and allowed to warm to room temperature and stirred for additional 2 h. Dimethyldichlorosilane (6.88 g, 53.3 mmol) was added into a different Schlenk flask equipped with addition funnel, diluted with 40 mL of THF, and cooled to 0 °C. The lithium salt of 1Me2PhInd was transferred into the addition funnel via cannula and slowly added (over 2.5 h) to the Me_2SiCl_2 solution at 0 °C. After addition was complete, the solution was allowed to warm to room temperature and was stirred overnight to give a clear, bright-yellow solution. All the solvents were removed in vacuo. The resulting brown-yellow oil was extracted three times with toluene. All the solvents were then removed in vacuo to obtain yellow oil. ^{1}H NMR (400 MHz, $CDCl_3$): −0.33 (3H), 0.17 (3H), 2.18 (3H), 4.06 (1H), 7.00−7.70 (m, 9H).

(3-Methyl-2-phenylindenyl)(2-phenylindenyl)dimethylsilane. The (3Me2PhInd)Me_2SiCl obtained in previous reaction was used without isolation and dissolved in 40 mL of THF in a Schlenk flask equipped with an addition funnel. 2-Phenylindene (2.66 g, 13.86 mmol) was dissolved in a separate Schlenk flask in 100 mL of THF and cooled to −78 °C. ^{n}BuLi (2.5 M in hexanes, 13.86 mmol) was slowly added to the 2PhInd solution via a syringe, and the solution was allowed to warm to room temperature and stirred an additional 2.5 h. The THF solution of the lithium salt of 2PhInd was added dropwise to the 3Me2Ph1Me_2SiCl at 0 °C over approximately 3 h. The solution was allowed to warm to room temperature and stirred under argon overnight. The reaction was quenched by the addition of an equal volume of saturated ammonium chloride solution. The organic layer was extracted once with water and twice with saturated sodium chloride solution. The aqueous layer was then extracted three times with diethyl ether. All the organic layers were combined, dried over $MgSO_4$, and filtered, and solvents were removed by a rotovap. The crude product was washed with cold hexanes. An off-white powder was filtered off and dried in the vacuum oven at 40 °C. Mixtures of isomers of the ligands were observed by ^{1}H NMR and were used in subsequent reactions without separation. Yield: 66% (3.205 g). ^{1}H NMR (500 MHz, $CDCl_3$): −1.11 (s, 3H), −1.10 (s, 3H), −0.93 (s, 3H), −0.80 (s, 3H), 2.255 (d, 3H, J = 2 Hz), 2.28 (d, 3H, J = 2 Hz), 3.81 (s, 3H), 3.88 (s, 1H), 4.27 (dd, 2H, J = 1.5, 7.5 Hz), 4.37 (s, 1H), 7.02 (s, 1H), 7.04 (s, 1H), 7.16−7.72 (m, H). Anal. Calcd for $C_{33}H_{30}Si$: C, 87.17; H, 6.65. Found: C, 87.42; H, 6.40.

***anti*-Dimethylsilyl(3-methyl-2-phenylindenyl)(2-phenylindenyl)zirconium Dichloride.** (3Me2PhInd)(2PhInd)-Me_2Si (2.5 g, 5.5 mmol) was suspended in 100 mL of diethyl ether. The suspension was cooled to −78 °C and ^{n}BuLi (2.5 M in hexanes, 11 mmol) added slowly via a syringe. The solution was allowed to warm to room temperature and stirred for an additional 2 h. $ZrCl_4$ (1.282 g, 5.5 mmol) was placed in a dry Schlenk flask and suspended in 130 mL of pentane. Both the lithium salt of the ligand and the suspension of zirconium tetrachloride were cooled to −78 °C. The lithium salt of the ligand was slowly added to the metal slurry via cannula, and the resulting solution was allowed to warm to room temperature and stirred overnight under an argon atmosphere in the dark. The suspension was then filtered via a Schlenk frit to give an orange solid and a clear orange solution. The orange solid was dried in vacuo and extracted with methylene chloride. The methylene chloride solution of the orange solid was concentrated and placed into a freezer at −40 °C for 4 days. Orange crystals were isolated. ^{1}H NMR shows pure *anti*-Me_2Si(3Me2PhInd)(2PhInd)$ZrCl_2$. Yield: 4% (140 mg). ^{1}H NMR (500 MHz, $CDCl_3$): 0.604 (3H), 0.892 (3H), 2.190 (3H), 6.52−6.86 (overlapping doublet of doublets, 4H), 7.007 (1H), 7.1−7.22 (b, 2H), 7.3−7.68 (overlapping multiplets, 12H). ^{13}C NMR (125 MHz, $CDCl_3$): 141.5, 141.1, 135.2, 133.9, 132.9, 132.8, 131.5, 128.6, 128.4, 128.0, 127.8, 127.5, 127.3, 127.2, 126.8, 126.4, 126.3, 126.2, 125.7, 125.7, 124.7, 120.1, 82.1, 81.8, 11.6, 5.3, 3.9. Anal. Calcd for $C_{33}H_{28}SiZrCl_2$: C, 64.47; H, 4.59. Found: C, 64.33; H, 4.57.

***syn*-Dimethylsilyl(3-methyl-2-phenylindenyl)(2-phenylindenyl)zirconium Dichloride.** The clear orange filtrate from the above reaction was dried in vacuo, and the solid was recrystallized from THF. It was then repeatedly recrystallized from toluene and a methylene chloride/pentane mixture. ^{1}H NMR shows pure *syn*-Me_2Si(3Me2PhInd)(2PhInd)$ZrCl_2$. Yield: 1% (39 mg). ^{1}H NMR (500 MHz, $CDCl_3$): 0.15 (3H), 1.52 (3H), 2.17 (3H), 6.80−6.88 (m, 4H), 7.03 (t, 2H), 7.10 (1H), 7.14−7.25 (overlapping multiplets, 6H), 7.38 (d, 1H, J = 9 Hz), 7.54 (d, 1H, J = 8.5 Hz), 7.60 (dd, 2H, J = 1.5, 7 Hz), 7.73 (d, 1H, J = 9 Hz), 7.88 (d, 1H, J = 8.5 Hz). ^{13}C NMR (125 MHz, $CDCl_3$): 3.1, 6.5, 11.5, 82.4, 82.4, 118.4, 124.4, 124.8, 125.0, 126.1, 126.5, 126.7, 127.0, 127.3, 127.5, 127.9, 129.9, 130.1, 130.8, 133.2, 134.3, 134.7, 135.7, 141.1, 141.6. Anal. Calcd for

$C_{33}H_{28}SiZrCl_2$: C, 64.47; H, 4.59. Found: C, 64.54; H, 4.74.

***anti*-Me$_2$Si(3Me2PhInd)(2PhInd)ZrMe$_2$.** Methyllithium (1.4 M diethyl ether, 0.651 mmol) was slowly added to an 80 mL diethyl ether suspension of *anti*-Me_2Si(3Me2PhInd)-(2PhInd)$ZrCl_2$ (200 mg, 0.325 mmol) at 0 °C. The solution was then allowed to warm to room temperature and stirred under nitrogen atmosphere overnight. The solution became clearer, but some insoluble orange solid was still present. This solution was filtered off, and the filtrate was dried in vacuo to yield yellow solid. This solid was extracted from methylene chloride to yield a deep orange solution. It was concentrated, layered with pentane, and left at room temperature for 6 h. Orange crystals that formed were used for X-ray structure determination.

X-ray Structure Determination of *anti*-Me$_2$Si(3Me2-PhInd)(2PhInd)ZrMe$_2$. A yellow-orange tablet crystal of $ZrSiC_{34.70}H_{33.10}Cl_{0.30}$ having approximate dimensions of 0.34 × 0.10 × 0.05 mm was mounted on a quartz fiber using Paratone N hydrocarbon oil. All measurements were made on a SMART[69] CCD area detector with graphite monochromated Mo Kα radiation. The structure was solved by direct methods[70] and expanded using Fourier techniques.[71] The non-hydrogen atoms were refined anisotropically. The expected formulation of the sample was pure $LZr(CH_3)_2$, but preliminary refinement against this model gave unacceptable thermal parameters and large residual electron densities for one of the methyl substituents (the remaining methyl group being well-ordered). Taking into account the synthesis of the molecule from a dichlorozirconium(IV) precursor, the asymmetric unit was accordingly modeled as a superposition of $LZr(CH_3)_2$ and $LZr(CH_3)(Cl)$ moieties, constitutionally disordered at a ratio of 7:3. Coordinates of the remaining, common atoms were highly correlated (correlation matrix element absolute values were larger than 0.95 in all cases) and unresolvable and were ultimately refined as belonging to a single common residue, with no detrimental effect on the *R* or goodness-of-fit indicators. Hydrogen atoms were located by difference Fourier but were fixed at idealized positions 0.95 Å from their parent atoms. All calculations were performed using the teXsan[72] crystallographic software package of the Molecular Structure Corp.

X-ray Structure Determination of (1Me2PhInd)-(2PhInd)ZrMe$_2$. An orange block crystal of $ZrCl_2C_{34.50}H_{28}$ having approximate dimensions of 0.23 × 0.15 × 0.11 mm was mounted on a quartz fiber using Paratone N hydrocarbon oil. All measurements were made on a SMART[69] CCD area detector with graphite monochromated Mo Kα radiation. The structure was solved by and expanded using Fourier techniques.[71] The non-hydrogen atoms in the main residue were refined anisotropically, while a toluene solvent molecule disordered over a 2-fold axis was refined first as a rigid group and ultimately held fixed in the final cycles. Hydrogen atoms were located by difference Fourier but were fixed at idealized positions 0.95 Å from their parent atoms. All calculations were performed using the teXsan[72] crystallographic software package of the Molecular Structure Corp.

Propylene Polymerization and Ethylene/Propylene Copolymerization. Polymerization grade ethylene from Praxair and liquid propylene from Amoco were used. Both monomers were further purified by passage through two columns packed with activated alumina and supported copper catalyst. Methylaluminoxane (MMAO type 4) from Akzo Nobel was dried in vacuo prior to use. Polymerizations were carried out in a 300 mL Parr reactor equipped with a mechanical stirrer. Temperature was maintained at 20 °C via an ethylene glycol/water cooling loop.

Propylene Homopolymerization. The reactor was flushed 3−4 times with gaseous propylene by pressurizing and venting and charged with liquid propylene (100 mL). The monomer was equilibrated at the reaction temperature, and the reaction was initiated by injecting the zirconocene/MAO solution in toluene (20 mL) under Ar pressure (250−300 psig × 30 mL) using a 50 mL injection tube. After 20 min, the reaction was quenched by injecting 20 mL of methanol; the reactor was slowly vented and opened. The polymer was precipitated in acidified MeOH (5% HCl), filtered, washed with methanol, and dried in a vacuum oven at 40 °C to constant weight.

Ethylene/Propylene Copolymerization. The reactor was flushed 3−4 times with gaseous propylene and charged with liquid propylene (100 mL). Propylene was cooled to the reaction temperature and overpressurized with ethylene to a certain total pressure. In a nitrogen drybox, an injector was charged with MAO dissolved in 17 mL of toluene, and the solution was injected into the reactor under ethylene pressure. 100 mL of propylene was added, and ethylene overpressure was used to supply ethylene into the reactor. This monomer mixture (toluene, MAO, propylene, ethylene) was equilibrated at the reaction temperature under constant ethylene pressure for at least 20 min. A catalyst stock solution was prepared in a drybox. The appropriate volume of catalyst solution was diluted with toluene to a total volume of 3 mL, added into a 10 mL injector, and injected into the reactor under ethylene pressure. Please note that, immediately prior to catalyst injection, the ethylene line was disconnected and the reactor was vented by 5 psi to provide the pressure differential and allow catalyst solution to flow into the reactor. The ethylene hose was reconnected directly after the catalysts injection. The reaction was run for 20 min at constant pressure and temperature; it was then quenched by injecting MeOH (20 mL), and the reactor was slowly vented and opened. The polymer was precipitated in acidified MeOH (5% HCl), filtered, washed with MeOH, and dried in a vacuum oven at 40 °C to a constant weight.

Polymer Characterization. Polymer molecular weights and molecular weight distributions were determined by high-temperature gel permeation chromatography using polypropylene for GPC calibration. A Varian UI 300 spectrometer was used to perform ^{13}C NMR measurements. Isotactic pentad content % [mmmm] of polypropylene samples was determined by dissolving 150−200 mg of polypropylene in 1,1,2,2-tetrachloroethane containing about 0.5 mL of 1,1,2,2-tetrachloroethane-d_2. An acquisition time of 1 s with no additional delays between pulses and continuous proton decoupling was used. Spectra were referenced using the [mmmm] peak. It was assumed that spin−lattice relaxation times and NOEs of all methyl groups were the same. Copolymer samples were prepared by dissolving 150−250 mg of each copolymer in 3 mL of *o*-dichlorobenzene/10 vol % benzene-d_6 with addition of paramagnetic "relaxation agent" chromium acetylacetonate [Cr(AcAc)] into a 10 mm tube. The spectra were measured at 120 °C using acquisition times = 1 s, additional delays = 5, and gated proton decoupling.

Acknowledgment. We acknowledge BP for financial support and for high-temperature GPC analysis. M.D. is the recipient of the Roche Bioscience Fellowship, for which she is grateful.

Supporting Information Available: Full pentad distributions for polypropylenes and triad distributions for ethylene/propylene copolymers produced with **2**, ***syn*-3**, ***syn*-4**, ***anti*-3**, and ***anti*-4**, a comprehensive copolymerization productivity data table for all catalysts, and X-ray crystal structure reports for **2** and ***anti*-4b**. This material is available free of charge via the Internet at http://pubs.acs.org.

References and Notes

(1) Resconi, L.; Cavallo, L.; Fait, A.; Piemontesi, F. *Chem. Rev.* **2000**, *100*, 1253−1345.
(2) Scheirs, J.; Kaminsky, W. *Metallocene-Based Polyolefins*; Wiley: Chichester, 2000; Vol. 1, 2.
(3) Natta, G.; Pino, P.; Corradini, P.; Danusso, F.; Mantica, E.; Mazzanti, G.; Moraglio, G. *J. Am. Chem. Soc.* **1955**, *77*, 1708−1710.
(4) Natta, G.; Mazanti, G.; Crespi, G.; Moraglio, G. *Chim. Ind. (Milan)* **1957**, *39*, 275−283.
(5) Natta, G.; Crespi, G. *J. Polym. Sci.* **1959**, *34*, 531−549.
(6) Natta, G.; Crespi, G. U.S. Patent 3,175,999, 1965.
(7) Kaminsky, W.; Buschermohle, M. U.S. Patent 4,841,004, 1989.

(8) Erker, G.; Muhlenbernd, T.; Benn, R.; Rufinska, A.; Tsay, Y. H.; Kruger, C. *Angew. Chem., Int. Ed. Engl.* **1985**, *24*, 321−323.
(9) Erker, G.; Nolte, R.; Kruger, C.; Schlund, R.; Benn, R.; Grondey, H.; Mynott, R. *J. Organomet. Chem.* **1989**, *364*, 119−132.
(10) Erker, G.; Nolte, R.; Tsay, Y. H.; Krueger, C. *Angew. Chem.* **1989**, *101*, 642−4.
(11) Erker, G.; Aulbach, M.; Knickmeier, M.; Wingbermuhle, D.; Kruger, C.; Nolte, M.; Werner, S. *J. Am. Chem. Soc.* **1993**, *115*, 4590−4601.
(12) Erker, G.; Mollenkopf, C.; Grehl, M.; Schonecker, B. *Chem. Ber.* **1994**, *127*, 2341−2345.
(13) Erker, G.; Nolte, R.; Aul, R.; Wilker, S.; Krueger, C.; Noe, R. *J. Am. Chem. Soc.* **1991**, *113*, 7594−602.
(14) Knuppel, S.; Faure, J. L.; Erker, G.; Kehr, G.; Nissinen, M.; Frohlich, R. *Organometallics* **2000**, *19*, 1262−1268.
(15) Dietrich, U.; Hackmann, M.; Rieger, B.; Klinga, M.; Leskela, M. *J. Am. Chem. Soc.* **1999**, *121*, 4348−4355.
(16) Okuda, J. *J. Organomet. Chem.* **1988**, *356*, C43−C46.
(17) Kaminsky, W.; Buschermohle, M. In *Stereospecific Polymerization of Olefins with Homogeneous Catalysts*; Fontanille, M., Guyot, A., Eds.; Reidel: New York, 1987; pp 503−514.
(18) Winter, A.; Antberg, M.; Rohrmann, J. U.S. Patent 4,962,-248, 1990.
(19) Coates, G. W.; Waymouth, R. M. *Science* **1995**, *267*, 217−219.
(20) Hauptman, E.; Waymouth, R. M.; Ziller, J. W. *J. Am. Chem. Soc.* **1995**, *117*, 11586−11587.
(21) Petoff, J. L. M.; Bruce, M. D.; Waymouth, R. M.; Masood, A.; Lal, T. K.; Quan, R. W. *Organometallics* **1997**, *16*, 5909−5916.
(22) Kravchenko, R.; Masood, A.; Waymouth, R. M. *Organometallics* **1997**, *16*, 3635−3639.
(23) Petoff, J. L. M.; Agoston, T.; Lal, T. K.; Waymouth, R. M. *J. Am. Chem. Soc.* **1998**, *120*, 11316−11322.
(24) Kravchenko, R.; Masood, A.; Waymouth, R. M.; Myers, C. L. *J. Am. Chem. Soc.* **1998**, *120*, 2039−2046.
(25) Lin, S.; Hauptman, E.; Lal, T. K.; Waymouth, R. M.; Quan, R. W.; Ernst, A. B. *J. Mol. Catal. A: Chem.* **1998**, *136*, 23−33.
(26) Kravchenko, R.; Waymouth, R. M. *Macromolecules* **1998**, *31*, 1−6.
(27) Leclerc, M. K.; Waymouth, R. M. *Angew. Chem., Int. Ed.* **1998**, *37*, 922−925.
(28) Tagge, C. D.; Kravchenko, R. L.; Lal, T. K.; Waymouth, R. M. *Organometallics* **1999**, *18*, 380−388.
(29) Lin, S.; Tagge, C. D.; Waymouth, R. M.; Nele, M.; Collins, S.; Pinto, J. C. *J. Am. Chem. Soc.* **2000**, *122*, 11275−11285.
(30) Nele, M.; Collins, S.; Dias, M. L.; Pinto, J. C.; Lin, S.; Waymouth, R. M. *Macromolecules* **2000**, *33*, 7249−7260.
(31) Collette, J. W.; Tullock, C. W.; MacDonald, R. N.; Buck, W. H.; Su, A. C. L.; Harrel, J. R.; Mulhaupt, R.; Anderson, B. C. *Macromolecules* **1989**, *22*, 3851−3858.
(32) Job, R. C. Shell Oil Co. U.S. Patent 5,118,767, 1990.
(33) Chien, J. C. W.; Llinas, G. H.; Rausch, M. D.; Lin, G. Y.; Winter, H. H.; Atwood, J. L.; Bott, S. G. *J. Am. Chem. Soc.* **1991**, *113*, 8569−70.
(34) Gauthier, W. J.; Corrigan, J. F.; Taylor, N. J.; Collins, S. *Macromolecules* **1995**, *28*, 3771−3778.
(35) Bravakis, A. M.; Bailey, L. E.; Pigeon, M.; Collins, S. *Macromolecules* **1998**, *31*, 1000−1009.
(36) Witte, P.; Lal, T. K.; Waymouth, R. M. *Organometallics* **1999**, *18*, 4147.
(37) Both catalyst precursors ***anti*-4** and ***syn*-4** are unstable in solid state and in solution and decompose within several days. Specifically, ***syn*-4** decomposes in the dark and at −40 °C within a few days which can be observed by decoloring of the bright orange solid to dull-greenish-orange color. In our case, catalysts stock solutions were prepared, and polymerizations were run within 4 days of isolating the compounds.
(38) Bruce, M. D.; Coates, G. W.; Hauptman, E.; Waymouth, R. M.; Ziller, J. W. *J. Am. Chem. Soc.* **1997**, *119*, 11174−11182.
(39) Kakugo, M.; Naito, Y.; Mizunuma, K.; Miyatake, T. *Macromolecules* **1982**, *15*, 1150−1152.
(40) Odian, G. *Principles of Polymerization*; John Wiley & Sons: New York, 1991.
(41) Knickmeier, M.; Erker, G.; Fox, T. *J. Am. Chem. Soc.* **1996**, *118*, 9623−9630.
(42) Pietsch, M. A.; Rappe, A. K. *J. Am. Chem. Soc.* **1996**, *118*, 10908−10909.
(43) Cavallo, L.; Guerra, G.; Corradini, P. *Gazz. Chim. Ital.* **1996**, *126*, 463−467.
(44) Coleman, B. D.; Fox, T. G. *J. Chem. Phys.* **1963**, *38*, 1065−1075.
(45) Schneider, N.; Schaper, F.; Schmidt, K.; Kirsten, R.; Geyer, A.; Brintzinger, H. H. *Organometallics* **2000**, *19*, 3597−3604.
(46) Petoff, J. L. M.; Myers, C. L.; Waymouth, R. M. *Macromolecules* **1999**, *32*, 7984−7989.
(47) Collins, S.; Gauthier, W. J.; Holden, D. A.; Kuntz, B. A.; Taylor, N. J.; Ward, D. G. *Organometallics* **1991**, *10*, 2061−2068.
(48) Lee, H.; Desrosiers, P. J.; Guzei, I.; Rheingold, A. L.; Parkin, G. *J. Am. Chem. Soc.* **1998**, *120*, 3255−3256.
(49) Nele, M.; Muqtar, M.; Xin, S.; Collins, S.; Dias, M. L.; Pinto, J. C. *Macromolecules* **2001**, *34*, 3830−3841.
(50) Maiti, A.; Sierka, M.; Andzelm, J.; Golab, J.; Sauer, J. *J. Phys. Chem. A* **2000**, *104*, 10932−10938.
(51) Kaminsky, W.; Schauwienold, A. M.; Freidanck, F. *J. Mol. Catal. A: Chem.* **1996**, *112*, 37−42.
(52) Steinhorst, A.; Erker, G.; Grehl, M.; Froehlich, R. *J. Organomet. Chem.* **1997**, *542*, 191−204.
(53) Naga, N.; Mizunuma, K. *Macromol. Rapid Commun.* **1997**, *18*, 581−589.
(54) Spaleck, W.; Aulbach, M.; Bachmann, B.; Kuber, F.; Winter, A. *Macromol. Symp.* **1995**, *89*, 237−247.
(55) Mallin, D. T.; Rausch, M. D.; Lin, Y. G.; Dong, S.; Chien, J. C. W. *J. Am. Chem. Soc.* **1990**, *112*, 2030−2031.
(56) Ewen, J. A.; Elder, M. J.; Jones, R. L.; Haspeslagh, L.; Antwood, J. L.; Bott, S. G.; Robinson, K. *Macromol. Chem. Macromol. Symp.* **1991**, *48/49*, 253.
(57) Ewen, J. A.; Elder, M. J.; Jones, R. L.; Curtis, S.; Cheng, H. N. *Stud. Surf. Sci. Catal.* **1990**, *56*, 439.
(58) Rieger, B.; Jany, G.; Fawzi, R.; Steimann, M. *Organometallics* **1994**, *13*, 647−53.
(59) Cheng, H. N.; Babu, G. N.; Newmark, R. A.; Chien, J. C. W. *Macromolecules* **1992**, *25*, 6980−6987.
(60) Llinas, G. H.; Dong, S. H.; Mallin, D. T.; Rausch, M. D.; Lin, Y. G.; Winter, H. H.; Chien, J. C. W. *Macromolecules* **1992**, *25*, 1242−53.
(61) Thomas, E. J.; Rausch, M. D.; Chien, J. C. W. *Organometallics* **2000**, *19*, 4077−4083.
(62) Monaco, G. *Macromolecules* **2001**, *34*, 4406−4415.
(63) Dankova, M.; Waymouth, R. M., manuscript in preparation.
(64) This conclusion assumes that the stereoselectivity of the unbridged rotamer is similar to that of the bridged metallocenes **4**.
(65) Copolymerizations were carried out in liquid propylene with an overpressure of ethylene in an effort to maintain a constant feed ratio; we felt it prudent to keep the overpressures below 200 psig which restricted us to compositions below 45% E incorporation.
(66) Lehtinen, C.; Lofgren, B. *Eur. Polym. J.* **1997**, *33*, 115−120.
(67) Reybuck, S. E.; Meyer, A.; Waymouth, R. M. *Macromolecules* **2002**, *35(3)*, 637−643.
(68) Arndt, M.; Kaminsky, W.; Schauwienold, A. M.; Weingarten, U. *Macromol. Chem. Phys.* **1998**, *199*, 1135−1152.
(69) *SMART: Area-Detector Software Package*; Siemens Industrial Automation, Inc.: Madison, WI, 1995.
(70) Altomare, A.; Cascanaro, M.; Giacovazzo, C.; Guagliardi, A. *J. Appl. Crystallogr.* **1993**, *26*, 343.
(71) Beurskens, P. T.; Admiraal, G.; Beurskens, G.; Bosman, W. P.; de Gelder, R.; Israel, R.; Smits, J. M. M. *The DIRDIF-94 program system, Technical Report of the Crystallography Laboratory*; University of Nijmegen: The Netherlands, 1994.
(72) *teXsan for Windows: Crystal Structure Analysis Package*; Molecular Structure Corporation: Woodlands, TX, 1997.

MA011486M